Review of Scientific Instruments

Sensitivity of MSE measurements on the beam atomic level population

Cite as: Rev. Sci. Instrum. **87**, 11E716 (2016); https://doi.org/10.1063/1.4959914
Submitted: 10 June 2016 . Accepted: 28 June 2016 . Published Online: 11 November 2016

C. Ruiz, S. T. A. Kumar, F. S. B. Anderson, and D. T. Anderson

AIP Publishing

Sensitivity of MSE measurements on the beam atomic level population

C. Ruiz,[a)] S. T. A. Kumar, F. S. B. Anderson, and D. T. Anderson
University of Wisconsin–Madison, Madison, Wisconsin 53706, USA

(Presented 9 June 2016; received 10 June 2016; accepted 28 June 2016; published online 23 August 2016)

The effect of variation in atomic level population of a neutral beam on the Motional Stark Effect (MSE) measurements is investigated in the low density plasmas of HSX stellarator. A 30 KeV, 4 A, 3 ms hydrogen diagnostic neutral beam is injected into HSX plasmas of line averaged electron density ranging from 2 to $4 \cdot 10^{18}$ m^{-3} at a magnetic field of 1 T. For this density range, the excited level population of the hydrogen neutral beam is expected to undergo variations. Doppler shifted and Stark split H_α and H_β emissions from the beam are simultaneously measured using two cross-calibrated spectrometers. The emission spectrum is simulated and fit to the experimental measurements and the deviation from a statistically populated beam is investigated. *Published by AIP Publishing.* [http://dx.doi.org/10.1063/1.4959914]

I. MOTIVATION

The MSE diagnostic technique is widely used for aiding in reconstructing profiles of current density and safety factor in plasma fusion devices. Both a polarimetry and full emission spectra method have been previously demonstrated.

A diagnostic neutral beam injects fast moving particles into the plasma which are mainly excited through electron collisions. Their emission is then collected, analyzed, and fit to a spectral model. The Doppler shifted emission is Stark split due to the Lorentz electric field experienced by the particles in their frame of reference.

The Stark multiplet emission line intensities are directly proportional to the atomic upper level populations. The spectra of MSE diagnostic technique rely on an accurate fit and identification of the individual emission lines. For this reason understanding of the beam population sublevels is of particular importance.

At densities on the order of 10^{20} m^{-3}, the beam is expected to reach a statistical equilibrium. Previous MSE measurements have shown deviations from the expected statistically populated sublevels.[1,2] The plasma density at the HSX quasi-symmetrical stellarator is two orders of magnitude lower and it is expected that deviations from statistically populated sublevels of the beam should be observed.

A synthetic diagnostic was developed to simulate and fit the beam emission spectra. The model is compared to ADAS[3] Stark module for validation purposes. Preliminary comparisons show good agreement between simulated synthetic data and modeling, giving confidence in applying the model to experimental data.

II. MSE DIAGNOSTIC ON HSX

The MSE diagnostic on HSX utilizes a set of diagnostic ports that were previously used for charge exchange recombination spectroscopy. The system is composed of a toroidal and a set of poloidal views of the plasma.[4] Of these views, only the toroidal view provides a large enough Doppler shift for measuring the Stark multiplet emission avoiding contamination from unshifted H_α and CII lines.

The diagnostic neutral beam at HSX has a maximum beam energy of 30 KeV, 4 A beam current and a neutralization efficiency of about 40%. With an effective pulse length of 3 ms, enough photons are recorded to be analyzed. Along the beam path, a low resolution spectrometer (0.1 nm/pxl) is used as a diagnostic tool for the beam.

The diagnostic system utilizes two spectrometers for simultaneous measurements of H_α and H_β emission lines. In order to compare their total emission line intensities, the spectrometers need to be cross-calibrated.

To cross-calibrate the spectrometers, the optical fibers connected to the vessel viewing ports are unplugged and connected to an integrating sphere. Many spectra are then collected and averaged; background light subtraction is performed with the integrating sphere turned off. By taking the ratio of the measured spectra we obtain a calibration factor which can then be applied to H_α and H_β emission lines for comparison.

III. BEAM EMISSION MODEL

A beam emission model was developed to simulate and fit H_α and H_β emission. The model is composed of two parts, beam into gas and beam into plasma for two of the Balmer series lines. The first part simulates the Doppler broadening and shift of the beam, and includes additional fractional beam energy components. The second part simulates the respective H_α and H_β Stark multiplet components. Experimental inputs when available are used for the simulations. The magnitude and direction of the magnetic field are obtained from VMEC.[5]

A. Beam into gas

To obtain a measurement of the broadening of the beam, a fit to beam into gas was performed. The broadening is due

Note: Contributed paper, published as part of the Proceedings of the 21st Topical Conference on High-Temperature Plasma Diagnostics, Madison, Wisconsin, USA, June 2016.
[a)]Electronic mail: carlos.ruiz@wisc.edu

to instrumental function, Doppler broadening, viewing geometry, and collection optics.

Using a neon pen lamp for wavelength calibration, the spectrometer's slit width was varied to determine optimal signal to noise ratio and resolution. For a slit width of 110 μm, we obtained an instrumental "temperature" of 0.22 eV.

From a fit to beam into gas a total "temperature" of 11.60 eV was obtained and is used for the width of each of the individual Stark emission lines. Moreover, the observed spectra showed a small but not negligible half-energy component which is taken into account for simulation and diagnostic purposes.

B. H_α - beam into plasma

The neutral beam injected particles are subject to a Lorentz electric field $\vec{E}_L = \vec{v} \times \vec{B} \sim 2.37 \times 10^6$ V/m and a radial[6] electric field at the core of HSX plasmas of $\vec{E}r \sim 40$ kV/m. Together they contribute to the Stark splitting of the beam energy levels.

The MSE emission spectra are the sum of different emission lines with their polarization parallel (π) and perpendicular (σ) to the total electric field. A total of 16 emission lines ($\pm\pi_8$, $\pm\sigma_6$, $\pm\sigma_5$, $\pm\pi_4$, $\pm\pi_3$, $\pm\pi_2$, $\pm\sigma_1$, $\pm\sigma_0$), of which 9 are resolvable, are used in the model.

The intensity of each transition line is modeled as $I = A_{ij} N_i \Phi(\theta)$ where A_{ij} is the transition probability,[7] N_i the number of particles in the upper level, and $\Phi(\theta)$ is the intensity dependence on the angle between line of sight and the total electric field. The total emission is modeled as a sum of Gaussian functions $y = \sum I \cdot e^{-(x-(\lambda+xd+xs))^2/xw^2}$, where λ is the H_α line, xs is the Stark split, xd is the Doppler shift, xw is the width of the Doppler broadened beam emission.

In Fig. 1 simulations including full and half-beam energy components are shown. The individual σ and π lines are seen to overlap due to the large Doppler broadening of the beam. A good agreement is found with ADAS Stark module. This gives confidence in applying the model to experimental data. In total the H_α model has six fitting parameters, five for the σ and π components, and one for the total intensity of the half-energy component.

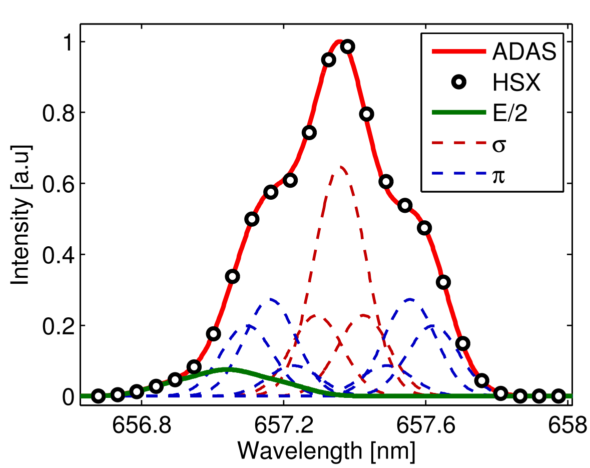

FIG. 1. Simulated ADAS and beam emission model data, half-beam energy component ($E/2$), and the individual σ and π features for the full energy component.

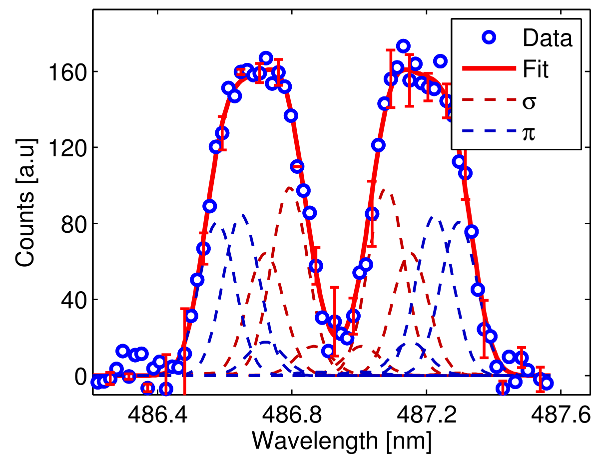

FIG. 2. Simulated H_β data with Gaussian noise and fit, included are the σ and π components.

C. H_β - beam into plasma

The H_β beam emission model is in principle similar to the H_α model. In this case the H_β Stark split is 44% smaller than H_α for HSX experimental parameters. The smaller split is compensated with the fact that the emission lines are separated twice as much giving 75% more spreading of the Stark multiplet.

There are 20 radiative transition lines ($\pm\pi_7$, $\pm\sigma_6$, $\pm\pi_5$, $\pm\sigma_5$, $\pm\pi_4$, $\pm\pi_3$, $\pm\sigma_3$, $\pm\sigma_2$, $\pm\pi_1$, $\pm\sigma_1$), of which three pairs radiate at the same wavelength. The intensity of each transition line is modeled as before. It has been shown that the number of independent fitting parameters can be reduced by identifying the lines that come from the same upper levels.[1]

Following a similar procedure, we reduce the number of fitted parameters for the H_β emission spectra. Specifically two groups of lines, one composed of π_4, σ_5, σ_3 originate from the upper level [201] in nkm notation, and another composed of π_3, π_1, σ_2 lines from [210] level. Our fitting model uses as independent fitting parameters the π_5, π_4, σ_2, σ_1 emission lines.

In Figure 2 we simulated with added Gaussian noise H_β emission spectra. The individual σ and π intensities were obtained from ADAS Stark module by choosing an artificially small beam temperature of 0.30 eV. The model was tested with simulated data and we were able to recover the individual σ and π emission intensities. The uncertainties of the fitting parameters are obtained using a bootstrap sampling method and the errors are propagated in the equations.

IV. EXPERIMENTAL MEASUREMENTS

In Figure 3 the experimental measurements of H_α beam into plasma and beam into gas are shown. An asymmetry of the Stark multiplet can be clearly seen. In the case of beam into gas with magnetic field the asymmetry is due to the half-beam energy component which accounts for 6% of the total Doppler

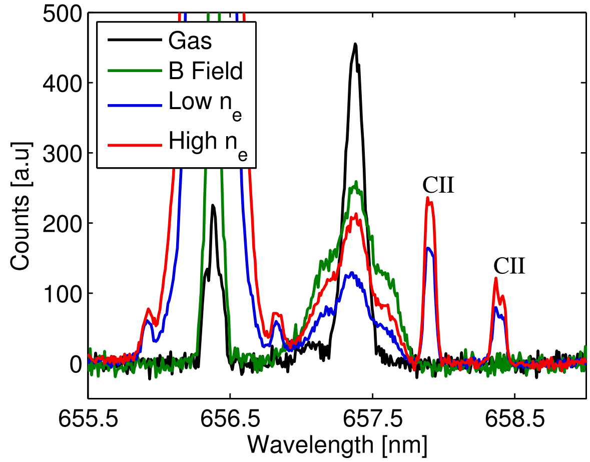

FIG. 3. Measured spectra of Doppler shifted H_α emission from: beam into gas, beam into gas with magnetic field, and beam into plasma at low and high densities (2-4·10^{18} m^{-3}).

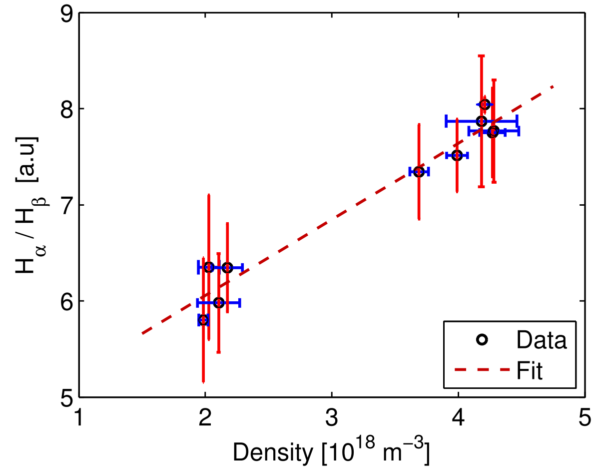

FIG. 5. Ratio of H_α/H_β emission as a function of density.

shifted emission. In the beam into plasma case the asymmetry is due to the half-energy component and to plasma impurity lines that radiate on top of the blue shifted wing of the Stark multiplet. A plasma background spectrum showed no impurity lines overlapping the red shifted wing of the Stark multiplet.

In Figure 4 the ratio of $\sum\sigma/\sum\pi$ from a fit to the H_α Stark split emission is shown. The results indicate a deviation from a statistically populated beam whose ratio of σ to π is close to 1. The results shown here could be affected by polarization dependent transmission coefficient of the diagnostic system setup. Further experimental measurements need to address this issue to confirm the results. The expected ratio obtained from ADAS simulations is within the data error bars.

In Figure 5 measurements of the line intensity ratio H_α/H_β are shown. Their ratio can be used to characterize the beam atomic populations. A linear relationship with density is clearly observed from the data. Although there is an offset in the experimental results the slope of the ratio is in agreement with ADAS simulations.

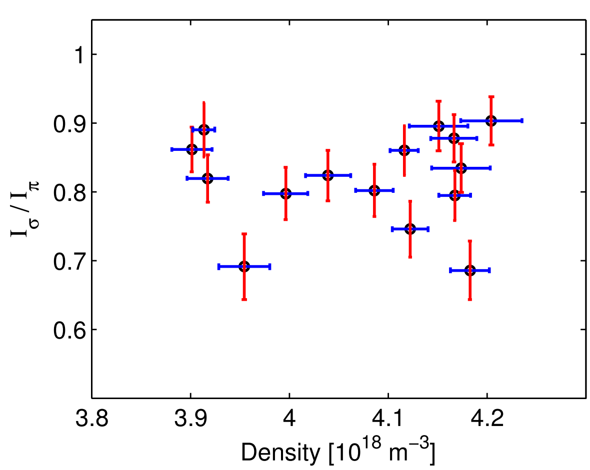

FIG. 4. Ratio of $\sum\sigma/\sum\pi$ emission as a function of density.

V. CONCLUSIONS

We developed simulation and fitting routines for the H_α and H_β Stark multiplet. The model was successfully compared to ADAS simulations. A set of synthetic data with artificial noise was generated and fitted with the model. Individual σ and π intensities of H_β emission were resolved using synthetic data.

Preliminary results of the ratio of $\sum\sigma/\sum\pi$ were found to deviate from statistical populated sublevels. Experimental measurements of the ratio of H_α/H_β total emission intensity follow the expected linear dependence in the HSX density range.

ACKNOWLEDGMENTS

This work was supported in part by the U.S. Department of Energy (DOE) under Grant No. DE-FG0293ER54222. Data for figures included in this publication are available for access at http://hsx.wisc.edu/HSXPublicationData.

[1] I. Bespamyatnov, W. Rowan, K. Liao, O. Marchuk, Y. Ralchenko, and R. Granetz, Nucl. Fusion **53**, 123010 (2013).
[2] W. Mandl, R. Wolf, M. G. von Hellermann, and H. P. Summers, Plasma Phys. Controlled Fusion **35**, 1373 (1993).
[3] H. P. Summers, http://www.adas.ac.uk (2004).
[4] A. Briesemeister, K. Zhai, D. Anderson, F. Anderson, and J. Talmadge, Plasma Phys. Controlled Fusion **55**, 014002 (2013).
[5] S. P. Hirshman and J. Whitson, Phys. Fluids **26**, 3553 (1983).
[6] J. Lore, W. Guttenfelder, A. Briesemeister, D. Anderson *et al.*, Phys. Plasmas **17**, 056101 (2010).
[7] N. Ryde, *Atoms and Molecules in Electric Fields* (Almqvist and Wiksell International, Stockholm, 1976).